Volume 1 | Number 1 | Jan 2013 | Pages 1–100

Journal of
Materials Chemistry B

Materials for biology and medicine
www.rsc.org/materialsB

ROYAL SOCIETY
OF CHEMISTRY

ROYAL SOCIETY
OF CHEMISTRY

www.rsc.org/materialsB

Journal Name

ARTICLE

Strongly fluorescent organogels and self-assembled nanostructures from pyrene coupled coumarin derivatives: Application in cell imaging

Krishnamoorthy Lalitha, Subbiah Nagarajan*

Three different coumarin coupled pyrene with varying hydrophobic unit (alkyl chains) has been synthesised and well characterized using NMR and mass spectral analysis. The gelation behaviour and self-aggregation properties of these compounds were studied relative to the molecular structure and solvent affinity. Among these derivatives, the one which is not having any hydrophobic tail displays efficient gelation in higher alcohols such as decanol and dodecanol. However the other derivatives having saturated and unsaturated hydrophobic tail forms weak gel in different solvents. The morphology of gel was investigated by optical microscopy and High Resolution Transmission Electron Microscopy (HRTEM). The investigation of absorption and emission spectra of these compounds revealed that the photo-physical properties were significantly influenced by self-assembly process in different solvents. The concentration dependent emission and ^{1}H NMR studies clearly suggest the π-π stacking interaction and hydrogen bonding between carbonyl groups of coumarin coupled pyrene with –OH group of solvent were the driving force for the process of gelation and self-aggregation. Rheological investigation clearly demonstrate the flow behaviour and reversible nature of organogel under temperature and strain ramp up and ramp down experimental conditions. By getting clue from self-assembly mechanism in different solvents, we derived nano flakes from coumarin coupled pyrene derivatives and further explored its potential application in the field of cell imaging. The size of the self-aggregated particles in DMSO-water mixture has been identified using HRTEM and zetasizer. The nanomaterials obtained via self-assembly process have used for fibroblast and PC3 prostate cancer cell imaging applications. Further investigation reveals that these compound supress the proliferation of PC3 cells.

Introduction

Supramolecular self-assembly is one of the fundamental techniques for the bottom-up fabrication of nanoscience. The self-assembly of small molecules to form diverse supramolecular architectures via various non-covalent interactions such as hydrogen bonding, π-π interaction, electrostatic and van der Waals interactions, hydrophilic-lipophilic balance (HLB) and other supramolecular weak forces has attracted substantial interest.[1] Self-assembled materials hold vast applications in the field of drug delivery, gene therapy, tissue engineering, enzyme immobilization, wound healing, water purification, biosensors and construction of novel nano- or microscopic materials and devices.[2] In this context low molecular weight organic gels (LMOGs) formed by the hierarchical assembly of gelators in a suitable solvent to structures such as fibrils, tapes, rods and tubes are known as an important class of soft materials.[2,3] In particular, LMOGs based on π-conjugated organic compounds have drawn significant interest due to their typical vantages such as diversity, flexibility, and promising applications in optoelectronics, light harvesting and energy materials.[4] Moreover these fluorescent gel systems show a remarkable variation in emission property which might be due to the phase transition process renders valuable information at molecular level self-assembly. Most frequently information on molecular level self-assembly renders opportunity to construct different nanostructures. Recent past there are number of fluorescent organogel with potential applications has been reported and same has been reviewed in detail by Ajayaghosh and co-workers.[5] With the intention of developing new fluorescent self-assembled

materials we put our extensive synthetic efforts to obtain more diverse pyrene-coupled coumarin based π-gelator with various hydrophobic tails, which could be used for biomedical and biological research. The self-assembled soft material i.e. gels derived from π-gelators are called "π-gels".[5,6] Π-Gels derived from naturally occurring fine chemical have received much attention because of their wide range of applications. Coumarin, a class of benzopyrone derivative falls under such category and has been used as an important pharmacophore for various diseases such as anticancer, antibacterial, antifungal, anticoagulant and anti-HIV agent.[7] In continuation with our ongoing research work in the field of self-assembled materials, herein we report a new class of π-gelator derived from renewable plant-derived resource, cashew nut shell liquid, which could self-assemble into gel form and nano flakes form in different solvents. Nowadays renewable resources have been vastly focused to establish and optimize efficient materials, biologically relevant molecules, and large-scale production of fine chemicals.[8] In the present report we have used cashew nutshell liquid (CNSL), an important by-product obtained from the cashew nut industry.[9] The major component of CNSL is a bio based non-isoprene lipid, cardanol which comprises a mixture of phenolic lipids: 5% of 3-*n*-pentadecylphenol (3-PDP), 50% of 3-(8*Z*-pentadecenyl)phenol, 16% of 3-(8*Z*,11*Z*-pentadecadienyl)phenol and 29% of 3-(8*Z*,11*Z*,14-pentadecatrienyl)phenol.[9]

Experimental section

General materials and methods

All chemicals used for the synthesis of coumarin derivatives (**3a-c**) and fluorescent probes (**5a-c**) were purchased from Sigma Aldrich, Merck, Alfa aesar and Avra chemicals and were used without further purification. All solvents were dried and freshly distilled before use. Solvents used for gelation studies are of AR grade. Double distilled water was used for preparing self-assembled nanostructures. Column chromatography was performed on Silica Gel (100-200 mesh) purchased from Avra chemicals, INDIA. Fibroblast L929 cell line was purchased from Sigma Aldrich and PC3 cells were obtained from National Centre for Cell Science (NCCS), Pune, India.

Characterization

^{1}H NMR and ^{13}C NMR spectra were recorded on Bruker 300 MHz NMR Spectrometer at 298 K. The ^{1}H and ^{13}C NMR chemical shifts were reported relative to TMS. Coupling constants (*J*) are denoted in *Hz* and chemical shifts (*δ*) in ppm. Proton multiplicity is assigned using the following abbreviations: singlet (s), doublet (d), triplet (t), quartet (q), multiplet (m). High resolution MS analyses were performed on an Agilent 6520 Q-TOF instrument by dissolving the solid sample in methanol.

Gelation method

A known quantity of gelator was mixed with appropriate amount of solvent in a sealed test tube, and the system was heated to 90-120 ºC until the solid was dissolved. By this procedure the solvent boiling point becomes higher than that under standard atmospheric pressure. The resulting solution was slowly allowed to cool to room temperature, and gelation was visually observed by inverting the test tube. A gel sample was obtained that exhibited no gravitational flow in inverted tube is denoted as "G". Instead of forming gel it remains as solution at the end of the tests is referred to as "S" (solution) and it remain as precipitate, the system was denoted as "P" (precipitation). The system, in which the gelator is not soluble even at the boiling point of the solvent, was called an insoluble system (I).

Gel-sol melting temperature (T_g).

Gel melting temperature was determined by flow of gel by test tube inversion method. All gels obtained are thermally reversible. Above their gelation temperature, the gel phase becomes solution phase, but could be returned to their original gel state upon cooling. Gel was prepared in a 5 mL glass vial as described above, the vial was immersed in the oil-bath 'upside down' and the vial is slowly heated. The temperature at which the gel melted down to solution was recorded as Gel melting temperature (T_g).

UV-Vis and Fluorescence measurements

UV/vis spectra were recorded on an Evolution 220 UV/visible spectrophotometer (Thermo Scientific). The spectra were recorded in the continuous mode between 200 and 700 nm, with a wavelength increment of 1 nm and a bandwidth of 1 nm. Emission spectra were measured on a JASCO spectrofluorometer FP-8200, by fixing the excitation value at 325 nm for dodecanol and DMSO. Selection of excitation value is based on the absorbance maximum of probes in different solvent. Samples for absorption and emission measurements were contained in 1 cm X 1 cm quartz cuvette.

Morphological analysis

Morphological analysis of gel formed by gelator was studied using Carl Zeiss AXIO ScopeA1 fluorescent/phase contrast microscope. A glass slide containing a small portion of gel was mounted on Phase Contrast Microscope and the morphology of gel was identified. Morphology of self-assembled structure such as gel and nano flakes were studied using JEOL JEM 2100 F FETEM.

Molecular modelling studies

MM2 energy minimised diagram was performed using ChemBio 3D Ultra 13. Red colour dotted line shows the possible hydrogen bond formation.

X-Ray diffraction studies

A small portion of a wet gel sample formed by gelator in decanol was transferred in a sample holder and coated like a

thin film. The XRD measurement was performed on XPert-PRO Diffractometer system.

Rheological measurements

The mechanical properties of gel were investigated with a stress controlled rheometer (Anton Paar 302 rheometer) equipped with a steel-coated parallel-plate geometry (25 mm diameter). The gap between two plates was 1 mm. The measurements were carried out at 23℃. Firstly, amplitude sweep measurement was conducted, which provides the information about linear viscoelastic range which is directly proportional to the mechanical strength of the gel sample. Secondly, the storage modulus, G' and the loss modulus, G" were monitored as functions of frequency sweep from 0.1 to 300 rad s^{-1}.

Cell proliferation assay

The anti-proliferation activity was tested by MTS assay on fibroblast L929 and PC3 cell line using the fluorescent dye, yellow tetrazolium dye, which when treated with cells, form purple coloured formazan product. The quantity of formazan is presumably directly proportional to the number of viable cells and is measured by using a spectrophotometer (1420-040 Victor 3 Multilabel Counter, PerkinElmer, USA) at 490 nm dissolved in PBS buffer. Viable cells with active metabolism convert MTT into a purple coloured formazan product. When cells die, they lose the ability to convert MTT into formazan, thus colour formation serves as a useful and convenient marker of only the viable cells. Cells were seeded into 96-well plate for 48 h prior treatment. They were then exposed to 40 μL of different concentrations (20, 40, 80 and 250 μg/1000 μL) of compounds, **5a-c** in 0.1% DMSO-water mixture and to control (0.1% of DMSO-water mixture). The relative viability was expressed as a percentage of the control well that was treated with the solvent 0.1% of DMSO-water mixture only. Cell viability (%) was estimated as a ratio of the absorbance of treated cell (N_t) to absorbance of untreated cells (solvent) (N_u) multiplied by 100.

$$\text{Cell viability (\%)} = (N_t / N_u) \times 100$$

Cell imaging/cell uptake studies

The Cell imaging / Cell uptake study of our fluorescent compounds **5a-c** were tested on Fibroblast L929 and PC3 cell lines. The cells were seeded into 6-well plate for 24 h prior treatment. They were then exposed to 40 μL of **5a-c** dissolved in in 0.1% DMSO-PBS buffer mixture with the concentration of 250 μg/1000 μL. After 4 h of exposure, the media were drained and the cells were washed with PBS buffer for more than 2 times. In order to differentiate the nucleus the Hoechst stain was then added and incubated for 15 minutes. After 15 min incubation, the stain was drained and the cells were again washed with PBS and subjected for imaging. The cells were imaged using confocal microscope.

Distillation of Cardanol

CNSL was distilled at a temperature between 210 and 280 °C, under a pressure of 2 to 8 mm Hg to get cardanol. Cardanol was

obtained as pale yellow liquid which darkens on further storage. After a second distillation, mixture of cardanol mono-, di- and tri-ene was obtained. Synthetic procedure for 3-pentadecyl phenol (hydrogenated cardanol), **1c** is as follows: To the solution of cardanol (10 mL) dissolved in dry methanol, 5% Pd/C was added slowly and the entire mixture was stirred in the presence of H$_2$ gas (1 atm) for 5h. After completion of reaction as identified using TLC, the solution was filtered through a celite bed to obtain crude 3-pentadecyl phenol. The pure product was obtained by recrystallization process using hexane as solvent.

Synthesis

General procedure for the *o*-formylation of substituted phenols

Dry paraformaldehyde (35 mmol) was added to a mixture of 3-alkyl phenol (4 mmol), anhydrous MgCl$_2$ (6 mmol) and triethylamine (15 mmol) in acetonitrile (25 mL) and the mixture was heated under reflux for about 12-15 h. After the completion of the reaction as identified by using TLC, the reaction mixture was cooled to room temperature and 5% aq. HCl was added. The crude product was extracted with ethylacetate, dried under Na$_2$SO$_4$ and purified using column chromatography.

Synthesis of cardanol-aldehyde (2b)

Dry paraformaldehyde (1.05 g, 35 mmol) was added to a mixture of cardanol (1.21 g, 4 mmol), anhydrous MgCl$_2$ (570 mg, 6 mmol) and triethylamine (2.1 mL, 15 mmol) in acetonitrile (25 mL) and refluxed for 15h. After completion of the reaction as identified by using TLC, the reaction mixture was cooled to room temperature and 5% aq. HCl was added. The crude product was extracted with ethylacetate, dried under Na$_2$SO$_4$ and purified using column chromatography using silica gel (hexane-ethylacetate, 98:2) to afford **2b** as yellow liquid. Yield = 88%.

^{1}H NMR (300 MHz, CDCl$_3$) δ: 0.88 (t, J = 6.9 Hz, 3H); 1.25-1.30 (m, 16H), 1.61-1.64 (m, 4H), 1.95-2.05 (m, 2H), 2.61 (t, J = 7.5 Hz, 2H), 6.80 (s, 1H), 6.83 (d, J = 8.1 Hz, 1H), 7.44 (d, J = 8.1 Hz, 1H), 9.83 (s, 1H), 11.05 (s, 1H). ^{13}C NMR (75 MHz, CDCl$_3$) δ: 195.81, 161.81, 153.84, 130.49, 130.01, 129.76, 120.51, 118.86, 117.08, 36.45, 32.62, 32.59, 31.94, 31.86, 31.80, 30.66, 29.72, 29.67, 29.54, 29.45, 29.34, 29.30, 29.25, 29.21, 29.16, 29.01, 28.91, 18.86, 27.24, 27.17, 14.12.

Synthesis of PDP-aldehyde, 2c

Dry paraformaldehyde (1.05 g, 35 mmol) was added to a mixture of 3-pentadecylphenol (1.22 g, 4 mmol), anhydrous MgCl$_2$ (570 mg, 6 mmol) and triethylamine (2.1 mL, 15 mmol) in acetonitrile (25 mL) and the mixture was refluxed for 15h. After completion of reaction as identified by TLC, the crude product was extracted with ethylacetate, dried under Na$_2$SO$_4$ and purified using column chromatography (hexane-ethylacetate, 96:4) to afford **2c** as white solid. Yield = 92%; mp = 53-56 ºC.

^{1}H NMR (300 MHz, CDCl$_3$) δ: 0.88 (t, J = 6.6 Hz, 3H), 1.25-1.59 (m, 26H), 2.61 (t, J = 7.5 Hz, 2H), 6.80 (s, 1H), 6.85 (d, J = 9.3 Hz, 1H), 7.45 (d, J = 7.8 Hz, 1H), 9.83 (s, 1H), 11.05 (s, 1H). ^{13}C NMR (75 MHz, CDCl$_3$) δ: 195.80, 161.81, 153.84, 120.50, 118.85, 117.08, 36.45, 31.94, 30.67, 29.71, 29.68, 29.55, 29.45, 29.38, 29.25, 22.71, 14.13.

General method for the synthesis of 3-acetyl-7-alkyl-2H-chromen-2-one, 3a-c.

To the compound **2a-c** (1 mmol) dissolved in ethanol, ethylacetoacetate (1.3 mmol), 0.3 mL of piperidine and 2-3 drops of glacial acetic acid were added. The mixture was refluxed for 4 h. After the completion of the reaction as identified by TLC, the reaction mixture was cooled to room temperature and 20 ml of ice cold water was added. The crude product was extracted with chloroform and dried over anhydrous Na$_2$SO$_4$ and purified using column chromatography using silica gel. Detailed synthesis of compound **3a** might be reported elsewhere.

Compound 3b: Yellow liquid; Yield = 82 %; ^{1}H NMR (300 MHz, CDCl$_3$) δ: 0.80 (t, J = 6.3 Hz, 3H), 1.14-1.24 (m, 16H), 1.56-1.60 (m, 4H), 1.90-1.96 (m, 2H), 2.65 (t, J = 8.1 Hz, 2H), 2.65 (s, 3H), 4.88-4.9 (m, 1H), 5.25-5.34 (m, 1H), 7.09 (d, J = 7.5 Hz, 1H), 7.1 (s, 1H), 7.47 (d, J = 8.1 Hz, 1H), 8.43 (s, 1H). ^{13}C NMR (75 MHz, CDCl$_3$) δ: 194.54, 158.52, 154.58, 150.44, 146.54, 128.97, 128.66, 124.64, 122.21, 115.09, 49.72, 44.25, 35.30, 30.9, 30.7, 29.81, 29.55, 28.68, 28.49, 28.34, 28.28, 28.11, 28.04, 27.96, 27.81, 27.28, 26.19, 26.11, 21.67, 21.63, 14.16.

Compound 3c: White solid; Yield = 89 %; ^{1}H NMR (300 MHz, CDCl$_3$) δ: 0.85 (t, J = 7.2 Hz, 3H), 1.18-1.32 (m, 24H), 1.59-1.67 (m, 2H), 2.71 (s, 3H), 2.72 (t, J = 6.9 Hz, 2H), 6.90-7.14 (d, J = 8.1 Hz, 1H), 7.17 (s, 1H), 7.54 (d, J = 7.8 Hz, 1H), 8.5 (s, 1H). ^{13}C NMR (75 MHz, CDCl$_3$) δ: 194.99, 158.96, 154.99, 150.88, 146.96, 129.35, 125.05, 122.62, 115.52, 115.49, 35.71, 21.29, 30.22, 20.97, 29.06, 29.02, 28.99, 28.89, 28.78, 28.73, 22.06, 13.49.

Synthesis of coumarin coupled pyrene derivatives (5a-c)

General procedure

To a solution of 3-acetyl coumarin (1 mmol) dissolved in 10 mL of n-butanol, 1-pyrenecarboxaldehyde (1.3 mmol), 3 drops of glacial acetic acid and 0.3 mL of piperidine was added and the contents were refluxed at 120 ℃ for 12 h. After completion of reaction as identified by TLC, the solvent was removed under vacuum. The residue thus obtained was triturated with 10ml of ethanol until the formation of fine precipitate. The precipitate was then filtered off and crystallized from methanol or ethanol.

Compound 5a

Yellow solid; Yield = 77 %; mp – 212-214 ℃; ^{1}H NMR (300 MHz, CDCl$_3$) δ: 7.47 (t, J = 7.5 Hz, 1H), 7.54 (d, J = 8.1 Hz, 1H), 7.79 (t, J = 7.5 Hz, 1H), 7.78 (d, J = 9.0 Hz, 1H), 8.0 (d, J = 6.6 Hz, 1H), 8.15 (t, J = 7.5 Hz, 1H), 8.24-8.41 (m, 6H), 8.59 (d, J = 8.4 Hz, 1H), 8.67 (d, J = 9.3 Hz, 1H), 8.79 (s, 1H), 8.89

(d, J = 15.6 Hz, 1H). HRMS (ESI+): m/z calcd for C$_{28}$H$_{16}$O$_3$ (M-H+2Li)$^+$ = 413.1320; observed = 413.2647.

Compound 5b

Yellow solid; Yield = 74 %; mp – 126-128 ℃; ^{1}H NMR (300 MHz, CDCl$_3$) δ: 0.81 (t, J = 4.5 Hz, 3H), 1.20-1.26 (m, 14H), 1.51-1.60 (m, 8H), 1.9-1.96 (m, 2H), 2.67 (t, J = 7.2 Hz, 2H), 5.26-5.32 (m, 2H), 7.11 (d, J = 7.8 Hz, 1H), 7.15 (s, 1H), 7.52 (d, J = 7.8 Hz, 1H), 7.94-8.17 (m, 7H), 8.20 (d, J = 15.6 Hz, 1H), 8.45 (d, J = 8.1 Hz, 1H), 8.54 (d, J = 9.3 Hz, 1H), 8.59 (s, 1H), 9.0 (d, J = 15.6 Hz, 1H). ^{13}C NMR (CDCl$_3$, 75 MHz) δ: 184.82, 158.41, 154.15, 149.88, 139.66, 131.77, 129.92, 129.34, 129.21, 128.41, 127.41, 127.32, 127.28, 126.06, 124.90, 124.73, 124.57, 124.39, 124.23, 123.82, 123.43, 123.22, 122.64, 121.25, 115.10, 114.72, 34.99, 29.50, 28.41, 28.32, 29.02, 27.91, 27.70, 21.37, 12.83. HRMS (ES+): m/z calcd for C$_{43}$H$_{45}$O$_3$ (M+Na)$^+$ = 632.3266; observed = 632.2545.
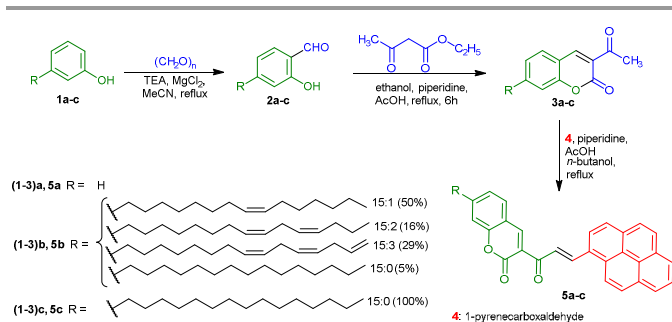
Compound 5c

Yellow solid; Yield = 82%; mp – 158-160℃; ^{1}H NMR (300 MHz, CDCl$_3$) δ: 0.88 (t, J = 6.3 Hz, 3H), 1.20-1.50 (m, 24H), 1.65-1.69 (m, 2H), 2.74 (t, J = 7.5 Hz, 2H), 7.19 (d, J = 7.8 Hz, 1H), 7.23 (s, 1H), 7.60 (d, J = 7.8 Hz, 1H), 8.02-8.16 (m, 3H), 8.19-8.25 (m, 4H), 8.20 (d, J = 15.6 Hz, 1H), 8.54 (d, J = 8.1 Hz, 1H), 8.62 (d, J = 9.3 Hz, 1H), 8.68 (s, 1H), 9.07 (d, J = 15.6 Hz, 1H). ^{13}C NMR (CDCl$_3$, 75 MHz) δ: 184.73, 18.25, 154.00, 149.77, 146.78, 139.54, 131.60, 129.75, 129.16, 129.05, 128.25, 127.24, 127.14, 127.11, 125.88, 124.71, 124.54, 124.38, 124.24, 124.10, 123.63, 123.39, 123.26, 123.06, 122.53, 121.08, 114.94, 112.59, 30.40, 28.17, 28.13, 28.01, 27.90, 27.84, 27.69, 21.17, 12.60. HRMS (ES+): m/z calcd for C$_{43}$H$_{47}$O$_3$ (M+Na)$^+$ = 634.3439; observed = 634.5325.

Results and discussion

Synthesis

Pyrene coupled coumarin derivatives that were designed for self-assembly studies are shown in Scheme 1. By complying electrophilic aromatic substitution reaction on phenol, we have synthesized both cardanol-aldehyde **2b** and PDP-aldehyde **2c**. The Knoevenagel reaction of compounds **2a-c** with ethyl acetoacetate under optimized reaction condition led to the formation of desired 3-acetylcoumarins **3a-c** in good yields. π-Gelators **5a-c** has been synthesized in good yields by aldol condensation of **3a-c** with 1-pyrenecarboxaldehyde **4** (Scheme 1). Here we have synthesised and completely characterized three different compounds with varying hydrophobicity and same has been utilized for self-assembly studies.

Scheme 1. Synthesis of pyrene coupled coumarin derivatives **5a-c**.

Table 1. Solvents/vegetable oils used for gelation studies

S. No	Solvent/vegetable oils	Observation (CGC % wt/v)[#]		
		5a	5b	5c
1	Ethanol	P	P	P
2	n-Butanol	PG	PG	P
3	Octanol	G (1.3)	G (1.3)	P
4	Decanol	G (0.28)	G (1.3)	P
6	Dodecanol	G (0.4)	G (1.0)	G (4.0)
7	Toluene	S	S	S
8	Benzene	S	S	S
9	1,2-Dichlorobenzene	S	S	S
10	Chloroform	I	I	I
11	Hazelnut oil	S	G (1.3)	P
12	Olive oil	S	G (1.3)	P
13	Heavy paraffin oil	PG	S	PG
14	Light paraffin oil	S	S	PG
15	Sesame oil	S	S	PG

[#] S = solution; P = precipitate; I = insoluble; G = gel; PG = partial gel.
Critical Gelation Concentration (CGC) is presented in parenthesis [% (w/v)]

Gelation studies

Supramolecular gelation is a process in which a pool of solvent molecules immobilized within highly entangled fibrous network obtained by the self-assembly of gelator.[10] Pyrene based low molecular weight organogelators (LMOG) are having a tendency to gelate solvents by using weak bonding mechanism.[11] Pyrene coupled coumarin, **5a** act as an excellent supramolecular gelator. Self-assembly of such an efficient gelator through non-covalent interactions into fibrillar aggregate that could immobilize the solvent molecule by capillary force to form a gel. Gelation ability of the gelator in aromatic solvents, alcohols and vegetable oils were summarized in Table 1. It is evident from table 1 that π-Gelators **5a** and **5b** exhibit excellent organogelation ability, showing critical gelation concentrations (CGCs) of 0.28 and 1.0 % (wt/v) respectively in higher alcohols such as decanol and dodecanol respectively. These gels were melted upon heating and form gel on cooling, hence they fall under the category of thermoreversible gel. In fact organogel formed by **5a** and **5b** experience a gel to sol transition upon heating-cooling cycles (T_g = 65℃). T_g increases with increase in concentration of gelator until it reaches the saturation point. Compound **5c** did not form gel in any of the tested solvent because of its enhanced hydrophobicity. Further detailed gelation test clearly shows that compound **5a-5c** do not form gel in any of the aromatic solvents tested and form stable gel in long chain alcohols and vegetable oils. Increasing the lipophilicity of the pyrene coupled coumarin derivatives by introducing unsaturated and saturated alkyl chain decreases the gelation ability.

Morphological analysis

Organogel: Morphology of gels were examined by using optical microscopy and HRTEM. Optical microscopy image of organogel obtained from **5a** in dodecanol is shown in Figure 1. All the structure clearly explains the formation of entangled thin fiber and twisted fiber-like structures with the dimension ranging between 100-200 nm (Figure 1). Figure 1a and b represents the optical microscopy image of gel formed by compound **5a** in dodecanol under white light. The inset in figure **1b** clearly depicts the formation of helical nano fibers. The fluorescence nature of self-assembled supramolecular structure has been identified by optical microscopy under fluorescence light. Figure 1c and 1d explains the fluorescence character of self-assembled fibres and twisted fibres. In order to have the further insight of gel, we have performed HRTEM analysis (Figure 1e and f). It should be remarked that width of the fiber or twisted fiber is higher than the molecular dimension of gelator **5a**. This result clearly depict that several gelator molecule self-assemble to form supramolecular architecture. Morphology and properties of the π-gel resembles the self-assembly mechanism of π-conjugated molecule.[5] Morphological studies reveals the formation of uniformly entangled fibrillar structure due to the hierarchical fashion of self-assembly of pyrene coupled coumarin derivative in highly cross-linked three dimensional supramolecular polymeric structure to form gel. Pictures of gel prepared in various solvents such as decanol, dodecanol and hazelnut oil under day light and UV light is shown in Figure 1g & 1h.
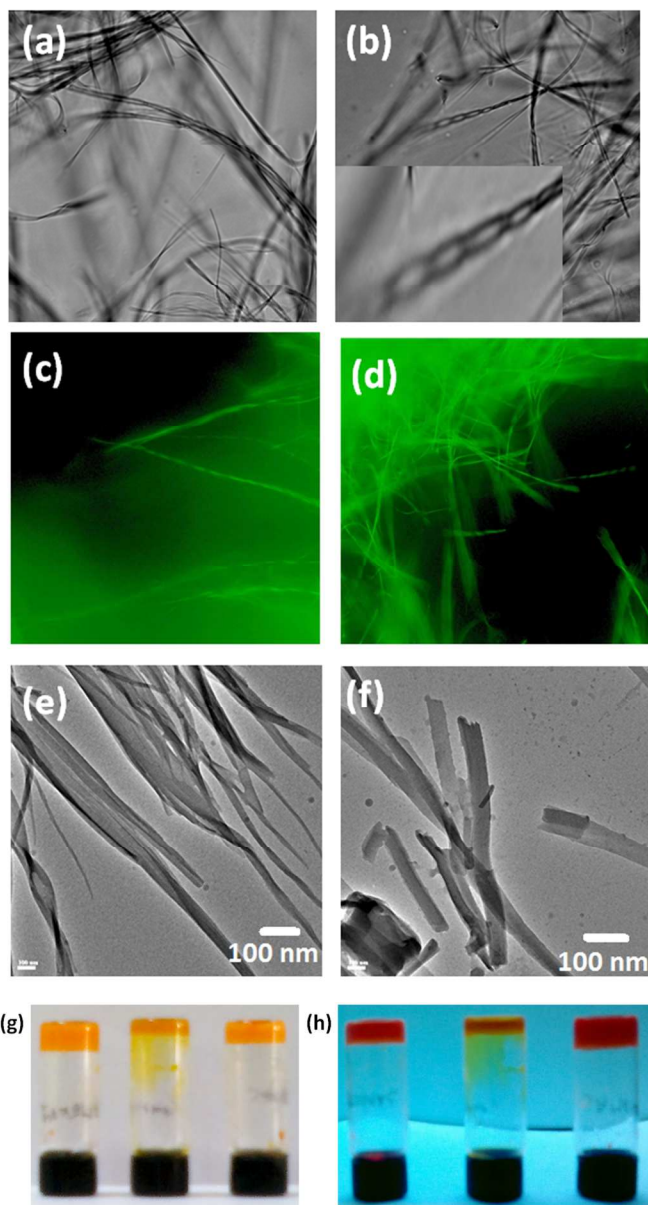
Figure 1. (a-d) Optical microscopy image of gel, **5a** in dodecanol (0.28 % wt/v) [(a & b) under white light (inset show the formation of twisted fibers); (c & d) under fluorescence light]; (e & f) HRTEM images of gel, **5a** in dodecanol; (g & h) Pictures of gel under day light and UV light respectively [left-**5a** in decanol, middle-**5b** in hazelnut oil and right-**5a** in dodecanol]

Self-assembled nano flakes: Since pyrene coupled coumarin, **5a** self-assemble to form gel in long chain alcohols, we were more interested in look on the self-assembly behaviour of gelator **5a** in water. Self-assembled nano flakes were prepared by refluxing the calculated amount gelator **5a** dissolved in 1:1 ratio of DMSO-water mixture followed by cooling at room temperature. On heating gelator **5a** got completely dissolved in solvent mixture and self-assembly has been induced by keeping the mixture undisturbed at room temperature. This resultant solution has been considered as stock solution and could be further diluted for cell imaging application. HRTEM analysis clearly depict the formation of nano flakes. This studies has

been extended to other compounds **5b** and **5c** also. Average size of nano flakes formed by **5a-c** in DMSO-water mixture (1×10^{-3}M solution) at lower concentration ranges between 10-100 nm (Figure 2).
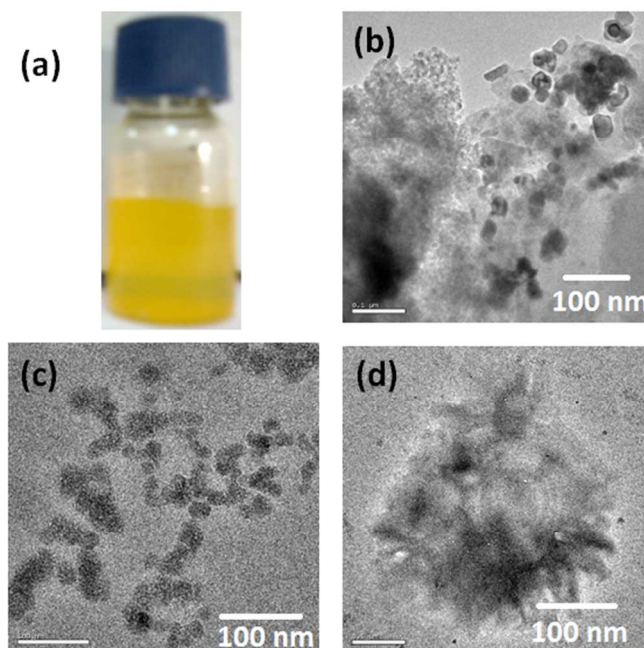

Figure 2. (a) Self-assembly of **5a** in DMSO-water (1:1 ratio; 1×10^{-3}M solution) (b-e) HRTEM images of the self-assembly of **5a**, **5b** and **5c** in DMSO-water mixture respectively.

^{1}H NMR studies

The supramolecular interaction of **5a** has been inferred by NMR spectral analysis. From ^{1}H NMR under the influence of different solvent, dilution and at different temperature could reveal both H-bonding and also the interaction between the aromatic moieties (π-π interaction). Solvent and or concentration dependent NMR studies for gelator **5a** has been performed to probe the driving force for the self-assembly process (Figure 3).
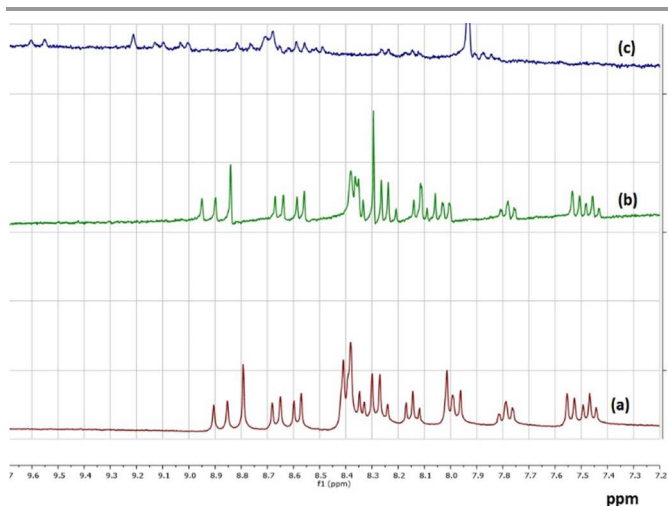
Figure 3. ^{1}H NMR spectra (aromatic region alone) of the compound, **5a**; (a) in DMSO-d_6; (b) in DMSO-d_6 + dodecanol (1:1 ratio); (c) in DMSO-d_6 + dodecanol (1:2 ratio).

The ^{1}H NMR spectra of compound **5a** shows clearly concentration dependent features. Resonance signal corresponding to the aromatic protons displayed a downfield shift with the increase in the concentration of gelator solvent. In non-gelling solvent (DMSO-d_6) aromatic protons showed signals between 7.45-8.90 ppm. Upon increasing the concentration of gelling solvent, these protons experience downfield shift and appears in between 7.85-9.60 ppm (Figure 3). It is well known phenomenon that the existence of π-π stacking in π-conjugated system shifts the aromatic protons more towards downfield. Thus the magnitude of π-π stacking in **5a** increases with increase in the concentration of gelling solvent.

XRD studies

X-Ray diffraction (XRD) experiment was employed to acquire an additional information about molecular packing of self-assembled **5a** in the gel state. Figure 4 shows the small angle XRD pattern of gel prepared from decanol. Small angle XRD of the gel provides a Bragg's reflection at 2.3 nm obtained from the packing of decanol due to the van der Waals interactions in gel network. The peak observed at 1.75 nm articulates coumarin coupled pyrene moiety. Bragg's reflection at 1.27 nm and 1.06 nm attributed to hydrogen bonded decanol with the carbonyl groups of pyrene-coupled coumarin derivative, **5a** (Figure 4a). This reflections are approximately equal to the molecular length of **5a** and hydrogen bonded decanol, which was confirmed by molecular modelling studies using energy minimized calculations. In addition XRD spectra of this gel show peak with position in the ratio of 1:2:3 suggest the existence of lamellar structure. Peaks appear at 0.37-0.48 nm are assignable to the (001) aspect of π-π stacking of aromatic units.[12] Based on the results obtained by NMR studies and XRD, we propose mechanism for the formation of self-assembled molecular gel (Figure 4b).
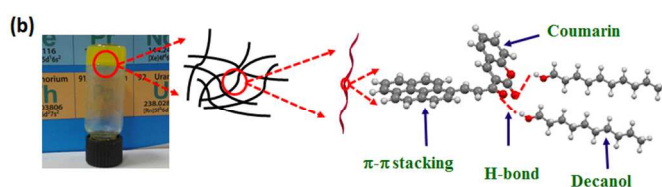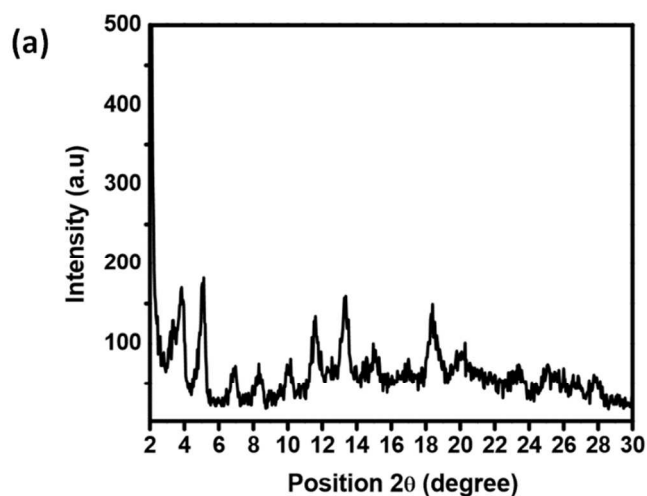

Figure 4. (a) SAXD data for gel prepared by **5a** in decanol and (b) proposed self-assembly mechanism.

Absorbance and emission studies

As discussed previously, π-conjugated fluorescent gel have attained more interest because of its potential applications especially in electronic and medical fields.[5,13] Accompanying the intention of studying the potential application in the field of medicine we have performed spectroscopic investigation on fluorescent organogel. The absorption spectrum of compound **5a** in different solvents such as acetonitrile, DMSO and dodecanol is shown in figure 5a. In acetonitrile solvent, compound **5a** show three bands centred at 307, 392 and 427 nm, which are assigned to un-aggregated form of coumarin and pyrene unit. The peak observed at 307 nm experience red shift and appeared at 352 nm by changing the solvent to DMSO. This red shift may be due to weak interaction of DMSO with coumarin core of **5a**. Absorption spectra of compound **5a** in dodecanol, a gelling solvent show red shift in all these peaks centred at 324 and 448 nm, which is due to molecular aggregation involving the formation of hydrogen bonding between carbonyl carbons coumarin moiety and dodecanol, π-π stacking of pyrene (Figure 5a). Molecular self-assembly of **5a** in higher alcohol has been clearly identified using UV-vis. Since gelator **5a** forms nano flakes in DMSO-water mixture, we intended to perform UV titration of compound **5a** dissolved in DMSO (1×10^{-5} M) with PBS buffer solution. Absorbance band for **5a** in DMSO solvent observed at 427 nm gradually decreases with sequential addition of 100μL of PBS buffer solution. The addition of PBS buffer to **5a** dissolved in DMSO resulted in the formation of self-assembled nano flakes (Figure 5a). The absorption spectra shift may take place either by solute

solvent interaction or solute-solute interaction induced by self-assembly or via chemical process such as charge transfer, proton transfer, etc. π-Conjugated molecule **5a** display higher molar extinction coefficient in the solvents tested clearly indicate the involvement of π-π* and n-π* transitions. Right after investigating the self-assembly features of **5a** to form gel and nano flakes using UV-vis spectroscopy, we have evaluated the fluorescence property. Under self-assembled state we could observe the intense fluorescence which stimulated us to further explore the emission property of compound **5a-c** under different experimental conditions. Emission spectra of compound **5a-c** displayed substitution dependence emission behaviour i.e. substitution on coumarin moiety slightly influence the emission property. Compound **5a** in dodecanol can self-assemble to form gel. In self-assembled state, emission spectrum of **5a** in dodecanol shows three peaks centred at 389, 409 and 554 nm. Dis-assembly has been induced by gradual addition of dodecanol, the intensity of peak observed at 409 nm got increased and peak centred at 554 nm showed blue shift. The observed significant blue shift of fluorescence maxima is mainly due to dis-assembly of self-assembled structure attained by titrating against dodecanol. (Figure 5b). Fluorescence emission spectra of **5a** was also measured in DMSO to look insight the effect of solvent. Compound **5a** in DMSO shows three intense peaks at 397, 409 and 478 nm, which is different from the peaks observed for dodecanol. The molecular aggregation of **5a** dissolved in DMSO was induced by

piecemeal addition of 100μL of PBS buffer. In aggregated state, the emission spectrum covers a broad range of visible spectral range and exhibit vibronic coupling maximum at 414 and 576 nm. The formation of self-assembled nano flake like structure has been identified by the drastic increase in emission intensity with a red shift (Figure 5c). We have also determined the fluorescence quantum yields of **5a-c** in different solvents ($1X10^{-5}M$). A very low fluorescence quantum yield ranging from 9-12 % has been observed for compound 5a-c in DMSO-PBS buffer (1:1 ratio), which could be due to the self-aggregation process. Quantum yields of 73% was observed in DMSO solvent alone. Similarly self-assembly of **5b** and **5c** was also identified by using UV and fluorescence studies (Figure 5d and 5e). Fluorescence of self-assembled system was not quenched even in extreme pH conditions (pH 4 & 10), and thus this system can be applied for cell imaging application under physiologically important conditions at various pH values. From these result, we resolve that at higher concentration, **5a** and **5b** self-assemble to form gel in decanol and dodecanol, and at lower concentration compounds **5a-c** self-assemble to form nanostructures such as nano-sheet and nano-flakes in DMSO-water (1:1 mixture). Since bio-applications of organogels were decently researched in the literature, we aimed to explore the possible application of self-assembled material i.e. nano flakes in cell imaging applications.
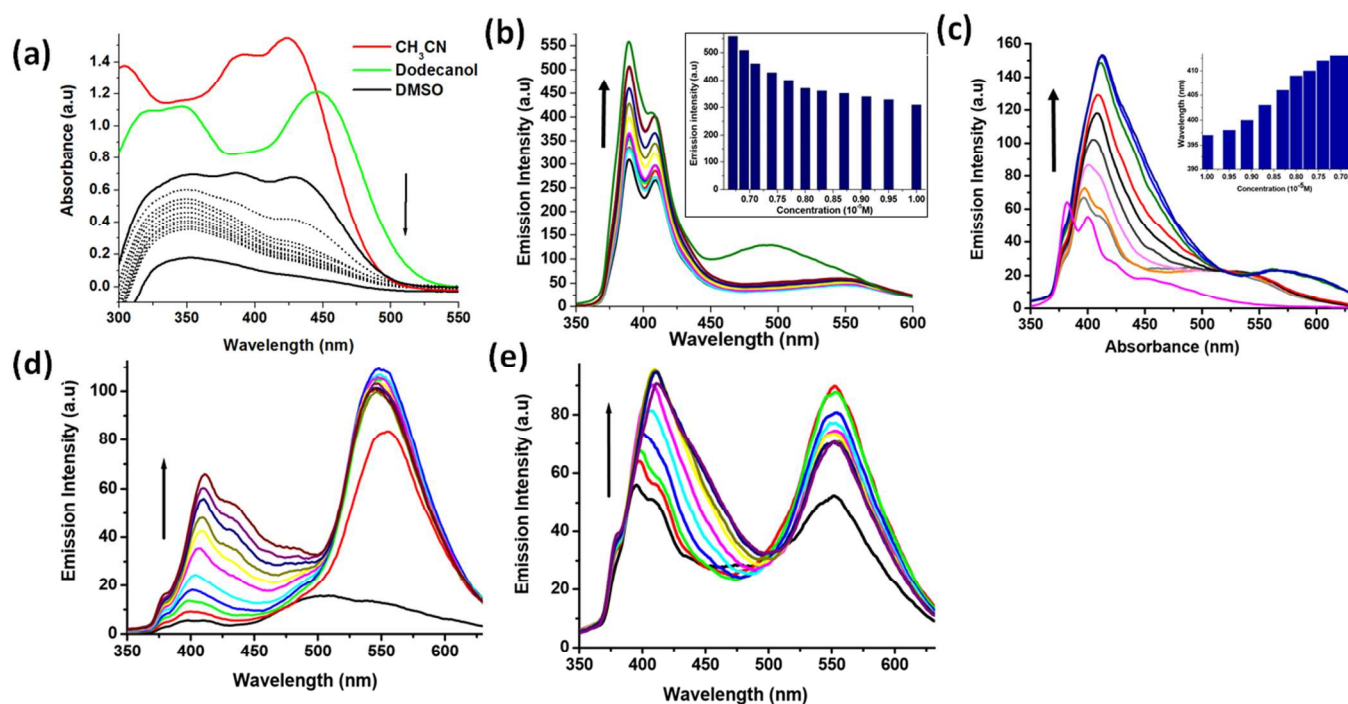

Figure 5. (a) UV-Vis spectra of **5a** in different solvents ($1X10^{-5}$ M), dotted line represents the UV titration of **5a** in DMSO with PBS buffer; (b) Emission spectra of **5a** in dodecanol and its response with respect to dilution, inset shows the plot of emission intensity vs concentration; (c) Fluorescence titration of **5a** in DMSO with PBS buffer and its corresponding plot of wavelength vs concentration; (d & e) Emission spectra of **5b** and **5c** in dodecanol respectively and its response with respect to dilution. In titration experiments, direction of arrow show the response of absorption and emission intensity with piecemeal addition of 100 μL of corresponding solvent. 2 mL of initial volume of solution ($1X10^{-5}M$) was taken for titration experiments.

Rheological studies

The elastic behaviour and flow characteristics of an organogel were determined by measuring rheology.[14] In frequency sweep experiment the variation of storage modulus (G′) and loss modulus (G′′) were monitored as a function of applied frequency at a constant strain of 0.1% at room temperature by using organogel prepared from compound **5a** in dodecanol at a concentration of 0.5% wt/v. Constant strain has been fixed by performing amplitude sweep. G′ represents the ability of deformed gel to restore its original geometry and G′′ represents tendency of gel to flow. For non-viscous liquid, G′ = 0 and for solids G′′ = 0. In viscoelastic material like gels, throughout the entire range of frequency sweep, the value of G′ was found to be more than that of G′′ (Figure 6a). G′and G′′ exhibited a very little frequency dependency with an increase in applied angular frequency. Thus visco-elastic deportment of gel was independent of frequency sweep, and this result suggesting that it possess good tolerance to external forces (Figure 6a). For organogel, at an angular frequency 0.1 rad/s, G′ in the order of magnitude 11 times greater than G′′. The rheological behaviour of a viscoelastic soft material is independent of strain up to a critical strain level (γc) and beyond γc, G′ start decline and the

material behaves in a non-linear fashion.[14] Figure 6b shows a strain sweep of organogel prepared by compound **5a** in dodecanol. With gradual increase in strain, G′ and G′′ remains constant and at a certain point gradual drop was observed and cross over occurs between G′ and G′′, the point at which the cross over occurs is considered as critical strain (γc) of a gel. The γc for organogel was found to be 2.73 (G′=G′′=490.7 Pa) (Figure 6b). Below γc (G′>G′′) gel behaves like a rigid solid, and this result clearly depict the formation of highly structured material, which could be disturbed by increasing the strain above γc, eventually become fluid-like. Continuous temperature ramp up and ramp down experiment clearly depict the stability of gel and hold back both structural and mechanical property even at elevated temperatures for more than three cycles (Figure 6c). Strain experiment demonstrate the exceptional mechanical behaviour of these gels which has been identified by simultaneously applying high and low magnitude of strain such as 100% and 0.1 % respectively. Under 100 % strain, both G′ and G′′ values were apparently decreased because of the broken network structure and recovery of G′ and G′′ was observed within 1-5 seconds by decline in strain to 0.1%. This result clearly arguing the reversible nature of gel and fast recovery of the mechanical property (Figure 6d).
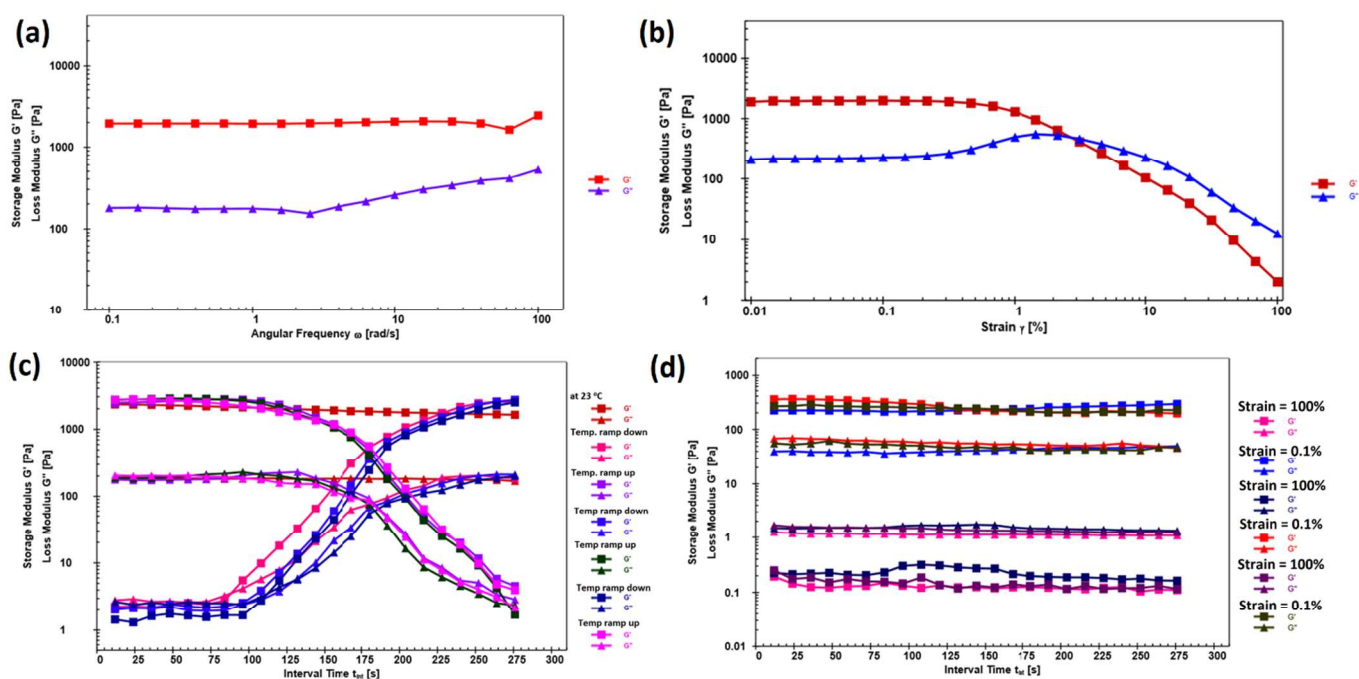

Figure 6. (a and b) Angular frequency and strain amplitude dependence of G′ and G′′ of organogel, **5a**; (c) Response of storage (G′) and loss modulus (G′′) of organogel with respect to temperature. Ramp up and ramp down temperature is 25-to-45ºC; (d) Time course change of G′ and G′′ of organogel in step strain condition 100% strain (4.5 min) and 0.1% strain (4.5 min) were applied alternatively. Concentration of SSG and MSSG: 0.5 wt/v% in dodecanol.

Cell imaging studies

The study on the effect of solvent in self-assembly process indicates that coumarin coupled pyrene derivatives can slowly assemble into fluorescent gel and nano flakes in different

solvent. The fluorescent nano flakes thus derived has been potentially used for cell imaging applications. Yao et. al. in his review clearly discussed the significance of combination of fluorescence and nanomaterials.[15] The recent development and innovation of fluorescent nanoparticles with unique optical

properties establish a new map for fluorescence imaging and sensing applications both *in vitro* and *in vivo*.[15] The use of organic fluorescent molecules possess more advantage of being much brighter and more stable than the fluorescent proteins. In addition the position of organic fluorescent molecules could be determined in precision than the fluorescent proteins. Most of applications such as *in vitro* and *in vivo* labelling in cells, tissues, and organisms, proteomic and genomic studies, disease diagnostics, pharmaceutical screening, drug delivery, assembled molecular control, protein purification, biological therapeutics, and medical imaging, sensing in cancer research, and selective tumor targeting rely on fluorescence spectroscopy.[16] Fluorescence imaging is one of the sensitive and most informative analytical techniques in modern research. Self-assembled nano flakes of **5a-c** formed in DMSO-water mixture could be potentially used for live cell imaging application. These nano particles of size between 10-100 nm are in the same range of dimension such as proteins, antibodies, membrane receptors, etc. These interesting characteristics, linked with their high surface to volume ratio impressed us to proceed further in this field. For our studies we have chosen fibroblast L929 cells and PC3 human prostate cancer cells. Medium has been prepared by dissolving 250µg of compound **5a-c** in 1000µL of solvent (0.1% DMSO-water mixture). Concentration of medium is as follows: **5a**: 0.6×10^{-3}M, **5b**: 0.4×10^{-3}M and **5c**: 0.4×10^{-3}M. At first we have studied the time dependent internalization of self-assembled nano flake formed by **5a**. Figure 7 clearly explains the internalization of self-assembled nanoparticle at different intervals such as 1 min, 5 min, 10 min and 2 h respectively. Then for further detailed investigation, cells were incubated with medium containing **5a-c** for 24 h. After incubation period, cellular localization was traced using Laser Confocal Scanning Microscopy (LCSM). The green fluorescence arising from self-assembled π-conjugated derivatives **5a-c** were clearly observed in the cytoplasm and perinuclear region of the cells. In compound **5a-c**, substituent at 7th position of coumarin moiety directly influence the fluorescence intensity. Compound **5a** is not having any substituent at coumarin core possesses more fluorescent character, whereas the other derivatives **5b** and **5c** are have alkyl substituent exert comparatively less fluorescence property (Figure 8).
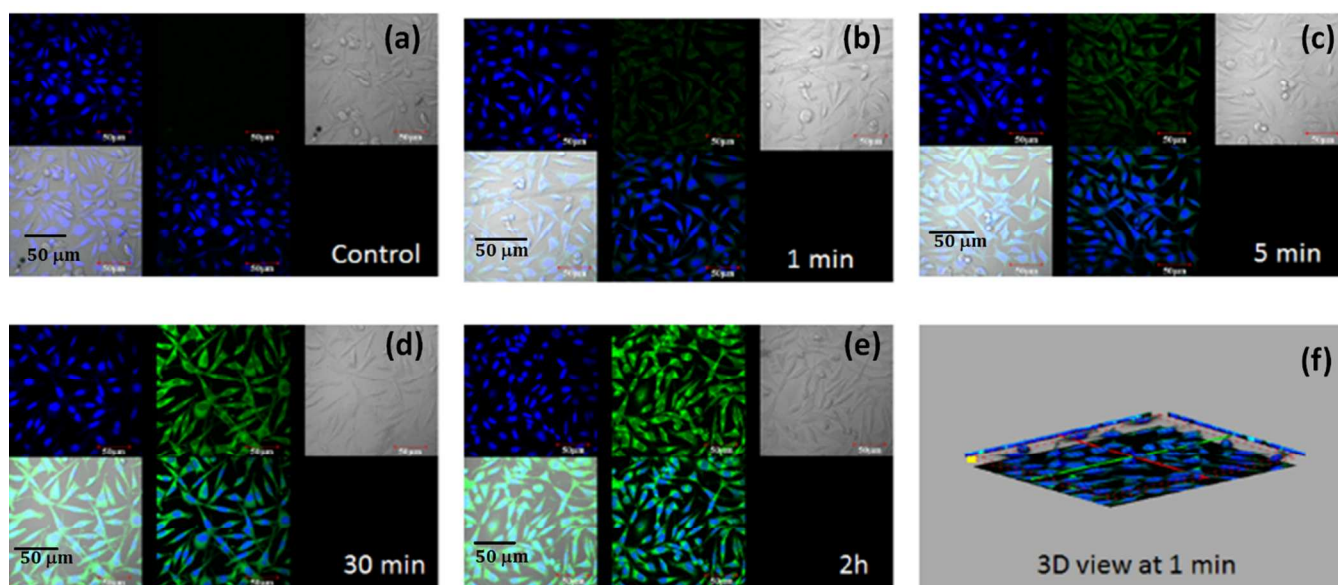

Figure 7. LCSM images of fibroblast L929 incubated with nano flake derived from **5a**. (a-e) Internalization of nanoparticle at 0 – 120 minute respectively; (f) 3D view of internalization of nanoparticle at 1 min. In figure 7a-e, top left: blue colour from Hoechst strain used to differentiate nucleus; Top middle: green fluorescence from cytoplasm and perinuclear region of the cells by fluorescent nanoparticle; bottom middle: combined view of blue and green colour fluorescence from nucleus, and cytoplasm and perinuclear region of the cells. Increase on intensity of green fluorescence in fibroblast L929 cells with respect to time is from self-fluorescent π-conjugated nano flakes derived from **5a**.[18]

It is interesting to note that among **5b** and **5c**, **5b** shows comparatively more fluorescent character. From this result one could say fluorescence intensity decreases with increase in hydrophobicity of π-conjugated systems (Figure 8). Nanoparticles/nano flakes prepared by self-assembly process from **5a-c** were uniformly located into the cytoplasm of the cells. The increase in incubation time enhance the uptake of fluorescent nano flakes. Endocytosis is the internalization of extracellular material via membranous vesicles.[17] Endocytic mechanism regulates how cells interact with their environment and it involves four different mechanisms such as Clathrin-mediated endocytosis, caveolae mediated endocytosis, macropinocytosis and phagocytosis. Inhibitors such as sucrose and chlorpromazine, blocking agents of clathrin-coated pit formation had no significant effect on cellular uptake and filipin, an inhibitor of caveolae-associated endocytosis) also had no significant inhibition effect on the nanoparticle uptake. Nocodazole, an inhibitor of macropinocytosis inhibited the

uptake of nanoparticle up to 60%. These results suggested that macropinocytosis and phagocytosis are the prominent cell

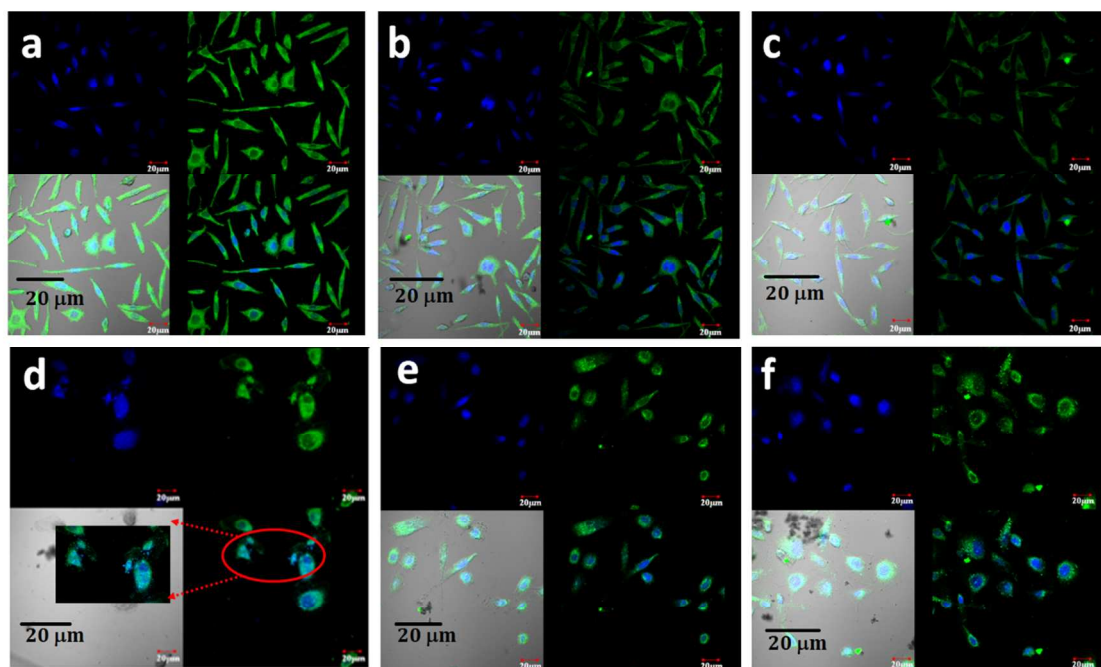uptake pathway for self-assembled nanoparticles.[18]

Figure 8. LCSM images of (a) fibroblast incubated with **5a**; (b) fibroblast incubated with **5b**; (c) fibroblast incubated with **5c;** (d-f) PC3 prostate cancer cells incubated with **5a-c** for 24h respectively. In figure 8a-f, top left: blue colour from Hoechst strain used to differentiate nucleus; top right: green fluorescence from and cytoplasm and perinuclear region of the cells fluorescent nanoparticle; bottom right: combined view of blue and green colour fluorescence from nucleus, and cytoplasm and perinuclear region of the cells. Rupture of cell membrane and overflow of cytoplasm could be directly identified from figure 8d-f [18]

We didn't observe any cell damage in fibroblast L929 on treatment with nano flakes, which entails the low cytotoxicity of nanoflakes in fibroblast. Cytotoxicity assay on both fibroblast and PC3 cells also supports the results obtained from LCSM. Treatment of PC3 cells with self-assembled nano flakes heads to the cell death in PC3 cells by inhibiting Wnt/β-catenin pathway, which has been identified based on cell membrane rupture and the overflow of cytoplasm (Figure 8d-f). Coumarin based anti-cancer drug, decursin inhibits Wnt/β-catenin pathway and cellular proliferation.[19] Cell proliferation or cell viability are good indicants of cell death. In order check the toxicity of compounds **5a-c**, we have examined cell viability towards fibroblast and PC3 cells. Fibroblast incubated with different concentrations of **5a-c** experience low cytotoxicity. Incubation of PC3 cells with different concentrations of **5a-c** show considerable cytotoxic effect (Figure 9). These self-fluorescent probes could be potentially used for optical diagnosis and treatment for prostate cancer.
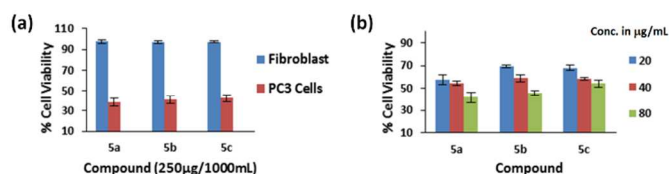

Figure 9. Graphical representation of (a) cell viability of fibroblast and PC3 cells when exposed to 250μg/1000μL of compound **5a-c**. (b) Cell viability of PC3 cells when exposed to increasing concentration of **5a-c** (20-80μg/1000μL). In fibroblast % of cell viability was around 95-98%

Conclusions

By utilizing aldol condensation as key step, a new class of pyrene coupled coumarin derivatives were successfully synthesised. Molecular structure of these compounds were completely characterized using NMR and mass spectral analysis. We have reported the formation of transparent fluorescent organogel with CGC of 0.28 % wt/v via supramolecular self-assembly through hydrogen bonding and π-π stacking of pyrene units. Morphology of organogel was investigated by optical microscopy and HRTEM. The concentration dependent absorbance and emission studies and ^{1}H NMR analysis reveal that hydrogen bonding between the carbonyl groups of **5a** and long chain alcohols, and π-π

stacking interactions were the driving force for the process of self-aggregation and gel formation. Optical property of π-conjugated derivatives has been strongly influenced by aggregation in different solvents, which resulted in redshift and increase in emission intensity. By getting clue from different modes of self-assembly in different solvents, we have prepared nano flakes in DMSO-water mixture. Under lower concentration compounds **5a-c** in DMSO-water forms nanoparticles (nano flakes) and at higher concentration forms gel in long chain alcohols and vegetable oils. The development of fluorescent organic functional nanoparticles has progressed exponentially over the past two decades because of its vast research in nanotechnology and considerable interest as feasible biomedical materials.[20] *In vitro* fluorescence imaging visualized the fluorescent emission from π-conjugated molecules in fibroblast L929 and PC3 prostate cancer cells. Although small molecular dyes used for imaging applications, the development of fluorescent multifunctional organic nanoparticle for *in vitro* fluorescent imaging offers powerful tool for many exciting applications. The continued evolution of these multifunctional self-assembled soft materials provide a promising platform for materials and medical applications.

Acknowledgements

Notes and references

ª Organic Synthesis Group, Department of Chemistry & The Centre for Nanotechnology and Advanced Biomaterials, School of Chemical and Biotechnology, SASTRA University, Thanjavur - 613401, Tamil Nadu, INDIA Fax: 04362264120; Tel: 04362304270; E-mail: nagarajan@scbt.sastra.edu.
Electronic Supplementary Information (ESI) available: [Emission spectra's and particle size analysis report]. See DOI: 10.1039/b000000x/

1. (a) S. Kinge, M. Crego-Calama and D. N. Reinhoudt, *Chemphyschem*, 2008, **9**, 20–42; (b) M. Giese, L. K. Blusch, M. K. Khan and M. J. MacLachlan, *Angew. Chem. Int. Ed. Engl.*, 2014, **54**, 2888–2910; (c) G. M. M. Sadeghi and M. Sayaf, *Nanostructured Polymer Blends*, Elsevier, 2014. 1   C. C. van den Akker, M. Schleeger, M. Bonn and G. H. Koenderink, *Bio-nanoimaging*, Elsevier, 2014; (d) J. Hamacek, *Metallofoldamers*, John Wiley & Sons, Ltd, Chichester, UK, 2013. 1   K. L. Morris and L. C. Serpell, *Amyloid Fibrils and Prefibrillar Aggregates*, Wiley-VCH Verlag GmbH & Co. KGaA, Weinheim, Germany, 2013; (e) K. Subramani and W. Ahmed, *Emerging Nanotechnologies in Dentistry*, Elsevier, 2012; (f) G. W. Padua and P. Nonthanum, *Nanotechnology Research Methods for Foods and Bioproducts*, Wiley-Blackwell, Oxford, UK, 2012; (g) K. Sugiyasu and S. Shinkai, *Supramolecular Polymer Chemistry*, Wiley-VCH Verlag GmbH & Co. KGaA, Weinheim, Germany, 2011.

2. (a) A. Kumar and V. Kumar, *Chem. Rev.*, 2014, **114**, 7044–7078; (b) M. Mauro, A. Aliprandi, D. Septiadi, N. S. Kehr and L. De Cola, *Chem. Soc. Rev.*, 2014, **43**, 4144; (c) T. Kato, N. Mizoshita and K. Kishimoto, *Angew. Chem. Int. Ed. Engl.*, 2005, **45**, 38–68; (d) S. Fleming and R. V. Ulijn, *Chem. Soc. Rev.*, 2014, **43**, 8150–8177; (e) P. G. Khalatur and A. R. Khokhlov, *Soft Matter*, 2013, **9**, 10943; (f) Y. Yang, Y. Zhang and Z. Wei, *Adv. Mater.*, 2013, **25**, 6039–49; (g) Y. Zhao, F. Sakai, L. Su, Y. Liu, K. Wei, G. Chen and M. Jiang, *Adv. Mater.*, 2013, **25**, 5215–56; (h) E. Busseron, Y. Ruff, E. Moulin and N. Giuseppone, *Nanoscale*, 2013, **5**, 7098–140; (i) Y. M. Chabre and R. Roy, *Chem. Soc. Rev.*, 2013, **42**, 4657–708; (j) H. Hofmeier and U. S. Schubert, *Chem. Commun. (Camb).*, 2005, 2423–32; (k) C. D. Simpson, J. Wu, M. D. Watson and K. Müllen, *J. Mater. Chem.*, 2004, 14, 494–504; (l) M.-C. Daniel and D. Astruc, *Chem. Rev.*, 2004, **104**, 293–346; (m) T. R. Cook, Y.-R. Zheng and P. J. Stang, *Chem. Rev.*, 2013, **113**, 734–77; (n) V. Balzani, A. Credi, F. M. Raymo and J. F. Stoddart, *Angew. Chemie - Int. Ed.*, 2000, 39, 3349–3391; (o) Z. Dong, Q. Luo and J. Liu, *Chem. Soc. Rev.*, 2012, **41**, 7890–908; (p) A. Winter, M. D. Hager, G. R. Newkome and U. S. Schubert, *Adv. Mater.*, 2011, **23**, 5728–48; (q) R. Chakrabarty, P. S. Mukherjee and P. J. Stang, *Chem. Rev.*, 2011, **111**, 6810–918; (r) A. Dawn, T. Shiraki, S. Haraguchi, S. Tamaru and S. Shinkai, *Chem. Asian J.*, 2011, **6**, 266–82; (s) H. K. Bisoyi and S. Kumar, *Chem. Soc. Rev.*, 2011, **40**, 306–19.

3. (a) T. Shimizu, M. Masuda and H. Minamikawa, *Chem. Rev.*, 2005, **105**, 1401–43; (b) C. Bai and M. Liu, *Angew. Chemie Int. Ed.*, 2013, **52**, 2678–2683; (c) A. Lakshmanan, S. Zhang and C. A. E. Hauser, *Trends Biotechnol.*, 2012, **30**, 155–65; (d) R. M. Iost and F. N. Crespilho, *Biosens. Bioelectron.*, 2012, **31**, 1–10; (e) B. Rybtchinski, *ACS Nano*, 2011, **5**, 6791–818; (f) K. Sakakibara, J. P. Hill and K. Ariga, *Small*, 2011, **7**, 1288–308; (g) S. S. Babu, H. Möhwald and T. Nakanishi, *Chem. Soc. Rev.*, 2010, **39**, 4021–35; (h) S. Cavalli, F. Albericio and A. Kros, *Chem. Soc. Rev.*, 2010, **39**, 241–263; (i) A. R. Hirst, B. Escuder, J. F. Miravet and D. K. Smith, *Angew. Chem. Int. Ed. Engl.*, 2008, **47**, 8002–18; (j) J.-H. Ryu, D.-J. Hong and M. Lee, *Chem. Commun.*, 2008, 1043–1054.

4. (a) V. K. Praveen, C. Ranjith, E. Bandini, A. Ajayaghosh and N. Armaroli, *Chem. Soc. Rev.*, 2014, **43**, 4222–42; (b) L.-H. Xie, S.-H. Yang, J.-Y. Lin, M.-D. Yi and W. Huang, *Philos. Trans. A. Math. Phys. Eng. Sci.*, 2013, **371**, 20120337; (c) H. Kobayashi, M. R. Longmire and P. L. Choyke, *Adv. Drug Deliv. Rev.*, 2013, **65**, 1112–9; (d) H. Kobayashi, M. R. Longmire and P. L. Choyke, *Adv. Drug Deliv. Rev.*, 2013, 65, 1112–9; (e) D. Türp, T.-T.-T. Nguyen, M. Baumgarten and K. Müllen, *New J. Chem.*, 2012, **36**, 282–298; (f) H. Detert and E. Sugiono, *Organosilicon Chemistry VI*, Wiley-VCH Verlag GmbH, Weinheim, Germany, 2005; (g) M. J. Hollamby, M. Karny, P. H. H. Bomans, N. A. J. M. Sommerdijk, N. A. J. M. Sommerdjik, A. Saeki, S. Seki, H. Minamikawa, I. Grillo, B. R. Pauw, P. Brown, J. Eastoe, H. Möhwald and T. Nakanishi, *Nat. Chem.*, 2014, **6**, 690–6; (h) F. Lu and T. Nakanishi, *Sci. Technol. Adv. Mater.*, 2015, **16**, 014805; (i) J. Zhang, C.-Z. Li, S. T. Williams, S. Liu, T. Zhao and A. K.-Y. Jen, *J. Am. Chem. Soc.*, 2015, **137**, 2167–2170; (j) L. K. Shrestha, R. G. Shrestha, Y. Yamauchi, J. P. Hill, T. Nishimura, K. Miyazawa, T. Kawai, S. Okada, K. Wakabayashi and K. Ariga, *Angew. Chem. Int. Ed. Engl.*, 2015, **54**, 951–5; (l) A. P. H. J. Schenning and S. J. George, *Nat. Chem.*, 2014, **6**, 658–9; (m) X.

Zhang, X.-D. Li, L.-X. Ma and B. Zhang, *RSC Adv.*, 2014, **4**, 60342–60348.

5. S. S. Babu, V. K. Praveen and A. Ajayaghosh, *Chem. Rev.*, 2014, **114**, 1973–2129.

6. C. Ren, J. Zhang, M. Chen and Z. Yang, *Chem. Soc. Rev.*, 2014, **43**, 7257–66.

7. (a) T.-F. Yeh, C.-Y. Lin, and S.-T. Chang, *J. Agric. Food Chem.* 2014, **62**, 1706; (b) S. Robert, C. Bertolla, B. Masereel, J.–M. Dogne and L. Pochwet, *J. Med. Chem.* 2008, **51**, 3077; (c) A. Maresca, C. Temperini, L. Pochet, B. Masereel, A. Scozzafava and C. T. Supuran, *J. Med. Chem.* 2010, **53**, 335-344.

8. (a) L. K. Aggarwal, P. C. Thapliyal and S. R. Karade, Progress in Organic Coatings, 2007, 59, 76; (b) T. Abhijit, J. Trissa and V. Vasant, U. S. Pat. Appl. Publ. 2012, US20120024527 A1 20120202; (c) A. L. M. Reddy, S. Nagarajan, P. Chumyim, S. R. Gowda, P. Pradhan, S. R. Jadhav, M. Dubey, G. John, and P. M. Ajayan, Sci. Rep. 2012, 2, 960. (d) G. John, B. V. Shankar, S. R. Jadhav and P. K. Vemula, Langmuir, 2010, 26, 17843; (e) C. Ding and A. S. Matharu, ACS Sustainable Chem. Eng., 2014, 2 (10), pp 2217–2236.

9. (a) V. S. Balachandran, S. R. Jadhav, P. K. Vemula and G. John, *Chem. Soc. Rev.* 2013, **42**, 427; (b) H. S. P. Rao, M. Kamalraj, J. Swain and A. K. Mishra, *RSC Adv.* 2014, **4**, 12175; (c) B. Lochab, S. Shukla and I. K. Varma, *RSC Adv.*, 2014, **4**, 21712; (d) C. Voirin, S. Caillol, N. V. Sadavarte, B. V. Tawade, B. Boutevin and P. P. Wadgaonkar, *Polym. Chem.*, 2014, **5**, 3142; (e) W. Kiratitanavit, S. Ravichandran, Z. Xia, J. Kumar and R. Nagarajan, *J. Renew. Mater.,* 2013, **1**, 289; (f) S. Kobayashi, H. Uyama and R. Ikeda, *Chem. Eur. J.* 2001, **7**, 4754; (g) L. Faure, S. Nagarajan, H. Hwang, C. L. Montgomery, B. R. Khan, G. John, P. Koulen, E. B. Blancaflor, and K. D. Chapman, *J. Biol. Chem.* 2014, **289**, 9340.

10. (a) R. G. Weiss, and P. Terech, *Molecular Gels, Materials with Self-Assembled Fibrillar Networks*, Springer, New York, **2006**; (b) B. Escuder, J. F. Miravet, *Functional molecular gels*, RSC soft Matter Series, **2014** and references cited there in.

11. (a) S. Nagarajan and T. M. Das, *New J. Chem.*, 2009, **33**, 2391; (b) K. Lalitha, K. Muthusamy, Y. S. Prasad, P. K. Vemula and S. Nagarajan, *Carbohydr. Res.*, 2015, **402**, 158–71.

12. G. John, G. Zhu, J. Li and J. S. Dordick, *Angew. Chem. Int. Ed.* 2006, **45**, 4772

13. (a) A. Ajayaghosh and V. K. Praveen, Acc. Chem. Res. , 2007, **40**, 644; (b) A. Ajayaghosh, V. K. Praveen and C. Vijayakumar, *Chem. Soc. Rev.* , 2008, **37**, 109.

14. (a) M. Laupheimer, N. Preisig and C. Stubenrauch, *Colloids Surfaces A Physicochem. Eng. Asp.*, 2015, **469**, 315–325; (b) M.-M. Su, H.-K. Yang, L.-J. Ren, P. Zheng and W. Wang, *Soft Matter*, 2015, **11**, 741–8; (c) S. Ghosh, R. Das Mahapatra and J. Dey, *Langmuir*, 2014, **30**, 1677–85; (d) D. Mandal, T. Kar and P. K. Das, *Chemistry*, 2014, **20**, 1349–58; (e) S. Liu, W. Yu and C. Zhou, *Soft Matter*, 2013, **9**, 864–874; (f) D. K. Maiti and A. Banerjee, *Chem. Asian J.*, 2013, **8**, 113–20; (g) X. Yu, X. Cao, L. Chen, H. Lan, B. Liu and T. Yi, *Soft Matter*, 2012, **8**, 3329; (h) B. Adhikari, J. Nanda and A. Banerjee, *Chemistry*, 2011, **17**, 11488–96; (i) G. Palui, A. Garai, J. Nanda, A. K. Nandi and A. Banerjee, *J. Phys. Chem. B*, 2010, **114**, 1249–56.

15. J. Yao, M. Yang and Y. Duan, *Chem. Rev.*, 2014, **114**, 6130–78.

16. (a) Q. Zheng, M. F. Juette, S. Jockusch, M. R. Wasserman, Z. Zhou, R. B. Altman and S. C. Blanchard, *Chem. Soc. Rev.*, 2014, **43**, 1044;

(b) S. van de Linde and M. Sauer, *Chem. Soc. Rev.*, 2014, **43**, 1076–87; (c) M. F. Juette, D. S. Terry, M. R. Wasserman, Z. Zhou, R. B. Altman, Q. Zheng and S. C. Blanchard, *Curr. Opin. Chem. Biol.*, 2014, **20**, 103–11; (d) Z. Zhao, J. W. Y. Lam and B. Z. Tang, *Soft Matter*, 2013, **9**, 4564; (e) J. Fan, M. Hu, P. Zhan and X. Peng, *Chem. Soc. Rev.*, 2013, **42**, 29–43; (f) H. Sahoo, *RSC Adv.*, 2012, **2**, 7017; (g) T. Ha and P. Tinnefeld, *Annu. Rev. Phys. Chem.*, 2012, **63**, 595–617; (h) J. Liu, X. Yang, X. He, K. Wang, Q. Wang, Q. Guo, H. Shi, J. Huang and X. Huo, *Sci. China Chem.*, 2011, **54**, 1157–1176; (i) J. O. Escobedo, O. Rusin, S. Lim and R. M. Strongin, *Curr. Opin. Chem. Biol.*, 2010, **14**, 64–70; (j) Z. Zhu, R. Yang, M. You, X. Zhang, Y. Wu and W. Tan, *Anal. Bioanal. Chem.*, 2010, **396**, 73–83; (k) H. Wang, E. Nakata and I. Hamachi, *Chembiochem*, 2009, **10**, 2560–77; (l) D. S. Y. Yeo, R. Srinivasan, G. Y. J. Chen and S. Q. Yao, *Chemistry*, 2004, **10**, 4664–72; (m) J. Riegler and T. Nann, *Anal. Bioanal. Chem.*, 2004, **379**, 913–9.

17. (a) M. Srinivasarao, C. V. Galliford and P. S. Low, *Nat. Rev. Drug Discov.*, 2015, **14**, 203–219; (b) A. Sharma, N. Jain and R. Sareen, *Biomed Res. Int.*, 2013, **2013**, 960821; (c) T. Balla, *Physiol. Rev.*, 2013, **93**, 1019–137; (d) C. Bechara and S. Sagan, *FEBS Lett.*, 2013, **587**, 1693–702; (e) J. Rauch, W. Kolch, S. Laurent and M. Mahmoudi, *Chem. Rev.*, 2013, **113**, 3391–406; (f) X.-Q. Zhang, X. Xu, N. Bertrand, E. Pridgen, A. Swami and O. C. Farokhzad, *Adv. Drug Deliv. Rev.*, 2012, **64**, 1363–84; (g) H. Mattoussi, G. Palui and H. Bin Na, *Adv. Drug Deliv. Rev.*, 2012, **64**, 138–66; (h) P. Debbage and G. C. Thurner, *Pharmaceuticals*, 2010, **3**, 3371–3416; (i) S. B. Fonseca, M. P. Pereira and S. O. Kelley, *Adv. Drug Deliv. Rev.*, 2009, **61**, 953–64; (j) P. M. Fischer, *Med. Res. Rev.*, 2007, **27**, 755–95.

18. K. Lalitha, P. Jenifer, Y. S. Prasad, K. Muthusamy, G. John and S. Nagarajan, *RSC Adv.*, 2014, **4**, 48433–48437.

19. (a) S.-J. Jeong, W. Koh, B. Kim and S.-H. Kim, *J. Ethnopharmacol.*, 2011, **138**, 652–61; (b) P. C. Leow, Z. Y. Ong and P.-L. R. Ee, *Curr. Chem. Biol.*, 2010, **4**, 49–63; (c) R. P. Singh and R. Agarwal, *Endocr. Relat. Cancer*, 2006, **13**, 751–78.

20. (a) K. Li and B. Liu, *Chem. Soc. Rev.*, 2014, **43**, 6570–97; (b) S. Bhattacharyya and A. Patra, *J. Photochem. Photobiol. C Photochem. Rev.*, 2014, **20**, 51–70; (c) M. Pastore and F. De Angelis, *Top. Curr. Chem.*, 2014, **352**, 151–236; (d) J. Gong, Q. Shen, Q. Fan and W. Huang, *Prog. Chem.*, 2013, 25, 1928–1941; (e) C. Zhang, Y. Yan, Y. Sheng Zhao and J. Yao, *Annu. Reports Sect. 'C' (Physical Chem.*, 2013, **109**, 211; (f) E. J. Harbron, *Isr. J. Chem.*, 2013, **53**, 256–266; (g) M. J. Ruedas-Rama, J. D. Walters, A. Orte and E. A. H. Hall, *Anal. Chim. Acta*, 2012, **751**, 1–23; (h) Y. Park and R. C. Advincula, *Chem. Mater.*, 2011, **23**, 4273–4294; (i) K. M. L. Taylor-Pashow, J. Della Rocca, R. C. Huxford and W. Lin, *Chem. Commun. (Camb).*, 2010, **46**, 5832–49; (j) K. M. L. Taylor-Pashow, J. Della Rocca, R. C. Huxford and W. Lin, *Chem. Commun. (Camb).*, 2010, **46**, 5832–49.

Abstract
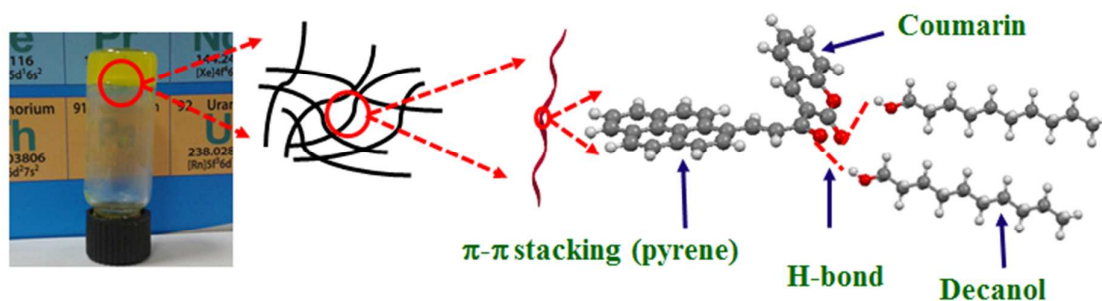
The present work reports facile synthesis of pyrene coupled coumarin derivatives which could form self-assembled molecular gel in long chain alcohols and nano flakes in aqueous medium. The morphology and physical properties of the organogel and nanoparticles were studied by HRTEM, absorbance and emission studies. Mechanical strength and reversible nature of organogel has been extensively studied using rheology. The nanomaterials obtained via self-assembly process could be potentially used in fluorescence imaging applications.